Anal Bioanal Chem (2015) 407:8813–8824
DOI 10.1007/s00216-015-9044-0

RESEARCH PAPER

Inter- and intra-organ spatial distributions of sea star saponins by MALDI imaging

Marie Demeyer[1,2] · Maxence Wisztorski[3] · Corentin Decroo[1] · Julien De Winter[1] · Guillaume Caulier[2] · Elise Hennebert[2] · Igor Eeckhaut[2] · Isabelle Fournier[3] · Patrick Flammang[2] · Pascal Gerbaux[1]

Received: 3 July 2015 / Revised: 3 September 2015 / Accepted: 10 September 2015 / Published online: 28 September 2015

Abstract Saponins are secondary metabolites that are abundant and diversified in echinoderms. Mass spectrometry is increasingly used not only to identify saponin congeners within animal extracts but also to decipher the structure/biological activity relationships of these molecules by determining their inter-organ and inter-individual variability. The usual method requires extensive purification procedures to prepare saponin extracts compatible with mass spectrometry analysis. Here, we selected the sea star *Asterias rubens* as a model animal to prove that direct analysis of saponins can be performed on tissue sections. We also demonstrated that carboxymethyl cellulose can be used as an embedding medium to facilitate the cryosectioning procedure. Matrix-assisted laser desorption/ionization (MALDI) imaging was also revealed to afford interesting data on the distribution of saponin molecules within the tissues. We indeed highlight that saponins are located not only inside the body wall of the animals but also within the mucus layer that probably protects the animal against external aggressions.

Keywords Saponin · Sea stars · Mass spectrometry · MALDI-mass spectrometry imaging

Electronic supplementary material The online version of this article (doi:10.1007/s00216-015-9044-0) contains supplementary material, which is available to authorized users.

✉ Maxence Wisztorski
maxence.wisztorski@univ-lille1.fr

✉ Patrick Flammang
Patrick.Flammang@umons.ac.be

✉ Pascal Gerbaux
pascal.gerbaux@umons.ac.be

[1] Organic Synthesis and Mass Spectrometry Laboratory, University of Mons—UMONS, 23 Place du Parc, 7000 Mons, Belgium

[2] Biology of Marine Organisms and Biomimetics, University of Mons—UMONS, 23 Place du Parc, 7000 Mons, Belgium

[3] Inserm U-1192, Laboratoire de Protéomique, Réponse Inflammatoire, Spectrométrie de Masse (PRISM), Université Lille 1, Cité Scientifique, 59655 Villeneuve D'Ascq, France

Introduction

Saponins are natural products first discovered in a large number of plants (e.g., *Quillaja saponaria*, *Dioscorea panthaica*) [1] and later in different marine organisms such as sea stars (asteroids) [2, 3], sea cucumbers (holothuroids) [4, 5], and sponges [6]. Holothuroid and sponge saponins are triterpene glycosides [7–10], while asteroid saponins are steroid glycosides [11, 12]. As reported in previous works, saponins are characterized by a large chemical diversity and a wide variety of pharmacological activities [1–6]. Because of the latter, these molecules have attracted considerable scientific interest, and their hemolytic, cytotoxic, antibacterial, antifungal, antiviral, and anti-tumor properties are already well documented [11, 13–19]. Paradoxically, their biological roles in marine animals are still very speculative [20]. Different studies have reported that saponins could play a role in several activities, being involved in chemical defense [7, 21] or in inter-specific chemical communication [22–24]. However, most of these studies were conducted using saponin mixtures extracted from whole animals, without taking into account the fact that saponin distribution is not homogeneous from one organ to another. In echinoderms, it was indeed observed that different organs are characterized by specific saponin contents, demonstrating that saponins are more than likely to fulfill biological roles associated with the containing organs or fluids [8, 25–29]. Based on these observations of organ-specific

saponin contents, it has been proposed that saponins could participate to digestion [25, 26], reproduction [28, 30], as well as chemical signaling [21–23, 31–33]. Finally, to our knowledge, only one study provides data associating one specific saponin to the physiology of the animal [34]. This molecule, known as Co-ARIS III (or ovarian asterosaponin 4), has been identified in the egg jelly of the sea star *Asterias amurensis* where it has been shown to participate to the acrosomial reaction during fertilization [34]. This literature survey demonstrates that the more precisely saponins are located in the animal tissues, the better their actual biological function can be inferred. In this connection, the analytical methods used in most studies, requiring the complete grinding of the organs to extract the saponin molecules, prevent determining the precise localization of the molecules within the tissue. During the last decade, the MALDI-MSI (matrix-assisted laser desorption/ionization-mass spectrometry imaging) method has been greatly developed to localize molecules of interest directly on a tissue section by recording mass spectra all across the tissue surface [35, 36]. The advantage of this technique is to obtain an accurate picture of the spatial distribution of molecules with a resolution that is now less than 50 μm. In addition, after MALDI-MSI analyses, the tissue section may still be analyzed by histological methods.

In the present paper, we selected *Asterias rubens*, a common sea star living in the northeastern Atlantic Ocean, as a model animal to demonstrate that direct MALDI-MSI analysis of saponins can be performed on the tissue without the need of time-consuming extraction and purification procedures. Three categories of saponins have been identified in sea stars, i.e., glycosides of polyhydroxysteroids, asterosaponins, and macrocyclic saponins [11, 26]. In *A. rubens*, only asterosaponins have been observed [27, 37]. As exemplified in Scheme 1, asterosaponins are pentaglycoside or hexaglycoside sulfated steroids that have high molecular weights (±1200 Da). The aglycone moiety is a $\Delta^{9,11}$-3β, 6α-dihydroxysteroid with a sulfate group at C3 and often an oxo function at C23 on the aglycone side-chain. The carbohydrate moiety is bound at the carbon atom C6 on the aglycone and includes five to six sugar residues. The most common monosaccharides are β-D-fucopyranose, β-D-quinovopyranose, β-D-xylopyranose, β-D-galactopyranose, and β-D-glucopyranose; 6-deoxy-xylo-hex-4-ulose (DXHU) and α-L-arabinopyranose are less frequently present. Previous researches have already identified 17 saponins in *A. rubens* by nuclear magnetic resonance (NMR) and mass spectrometry (MS) [12, 37–43]. More recently, we detected nine new molecules by mass spectrometry and we also analyzed with great care their inter-organ distribution paying attention to five different organs, namely the aboral body wall, the oral body wall (including tube feet), the stomach, the pyloric caeca, and the gonads [27]. All the collected data indicated that each organ is characterized by a specific mixture of saponins. However, the saponin extraction protocols used precluded any further localization of the congeners in the tissues. The present work is a proof-of-principle study aiming to demonstrate the feasibility of MALDI-MSI to analyze saponin molecules on sea star tissues. For this purpose, we recorded on-tissue MALDI mass spectra which were shown to reproduce the MALDI-TOF data obtained on the extracts. Moreover, MALDI-MSI methods were also demonstrated to afford data on the distribution of saponin molecules within the tissue. In this context, we also report that carboxymethyl cellulose can be advantageously used to fill empty cavities of the animal to facilitate the cryosectioning procedure [44]. This is clearly evidenced for sea stars whose arms are difficult to cut because their body wall comprises calcareous ossicles. For the present study, we deliberately selected animals collected at different stages of the reproductive cycle to try covering a large panel of different physiological states. However, the quite limited data will definitively prevent us from performing statistical analyses that are necessary to associate the localization of saponins with their biological activities. To probe the analytical reproducibility of the method, we will associate the newly obtained MALDI data with results obtained by mass spectrometry analyses of saponin extracts [27]. Additionally, we will use the measure of hemolytic activity as an orthogonal, non-MS based method to access saponin concentrations on tissue extracts [27]. This paper will therefore pave the way for future and more systematic studies that could be conducted to understand the biological roles of saponins in the sea star *A. rubens* and other echinoderms.

Materials and methods

Chemicals

For saponin extractions (see Electronic Supplementary Material (ESM) for details [8]) and mass spectrometry analyses, technical grade methanol, hexane, dichloromethane, chloroform, and isobutanol, as well as the HPLC grade water, acetonitrile, and methanol, were purchased from CHEM-LAB NV (Somme-Leuze, Belgium). Amberlite XAD-4, dimethylaniline (DMA) and 2,5-dihydroxybenzoic acid (DHB) were provided by Sigma-Aldrich (Diegem, Belgium). For the MALDI-MSI analyses, HPLC grade water and AR grade trifluoroacetic acid (TFA) were obtained from Biosolve B. V. (Valkensvaard, The Netherlands). Methanol (MeOH), DHB, and DMA were purchased from Sigma-Aldrich (Saint-Quentin Fallavier, France).

Sampling and sea star selection

Individuals of *A. rubens* Linnaeus, 1758, were collected on boulders during low tide at Audresselles (Opal Coast, France)

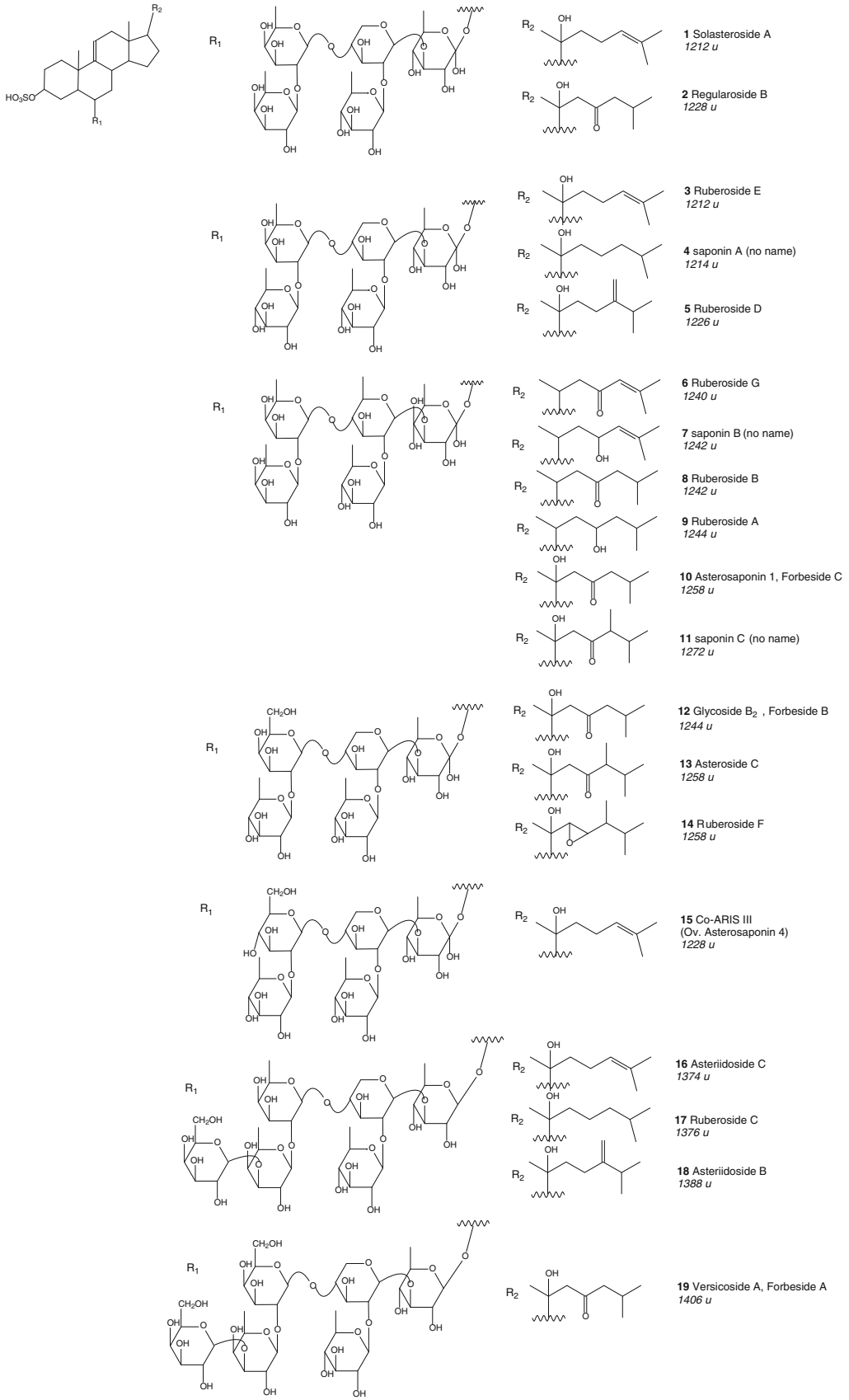

Scheme 1 Asterosaponins from *Asterias rubens* [37–43]

at four different periods: (i) in winter (March 12, 2012), (ii) in summer (September 19, 2012), (iii) winter (February 06, 2014), and (iv) in spring (June 15, 2014). They were transported to the Laboratory of Biology of Marine Organisms and Biomimetics at the University of Mons, where they were kept in a marine aquarium with closed circulation (13 °C, 33 psu). Amongst the collected animals, one individual for each of the four sampling periods was selected for the MALDI-MSI analyses. For the mucus analysis, 20 sea stars (June 2014) were selected. Practically, to collect mucus produced by the oral and aboral body wall, the individuals were placed upside down in glass Petri dishes and stressed by shaking [45]. The oral and aboral mucus were collected separately by suction using a glass pipette connected to a Buchner flask maintained under a slight vacuum. The collected materials were stored at 4 °C before further analysis. Two additional animals (June 2014) were sacrificed for qualitative (mass spectrometry) and quantitative (hemolytic activity—see ESM) analyses of body wall saponins, with and without mucus removal. Animals used in our experiments were maintained and treated in compliance with the guidelines specified by the Belgian Ministry of Trade and Agriculture.

Tissue preparation for on-tissue MALDI and MALDI-MSI

The preparation of transverse cryosections through a sea star arm is particularly difficult to achieve because their body wall comprises many calcareous ossicles. This task is even more difficult when the organs present in the arm, i.e., the gonads, are not sufficiently developed, leaving large fluid-filled volumes free of organs within the arm which therefore collapses during sectioning. This is for instance the case during the summer season [46]. Moreover, besides the crushing of the arm, organs are also expected to move or to overlap during the cryosectioning procedure. In this context, we decided to investigate methods to enhance tissue stabilization during sectioning. A solution of carboxymethyl cellulose (CMC) (2 % in water) was injected within the arm after dissection [44]. The dissected sea star arm was filled with the CMC solution using a Pasteur pipette. The filled arm was then immersed horizontally in an aluminum homemade mold also containing the CMC solution. Air was removed by slightly pressing the arm. The entire mold was plunged in a container filled with isopentane cooled by liquid nitrogen. After 20 min of freezing, the mold was removed and the block containing the arm was mounted onto a cryostat freeze plate at −25 °C for at least 30 min. The block was cut transversely into thick slices which were fastened to the specimen holder with a small amount of Tissue-Tek OCT (Fisher Scientific), ensuring that the surface to be sectioned does not contact the OCT to avoid polymer interferences. Sections were made in the proximal part of the arm, near the central disk of the animal, in order to be sure to observe all the organs present in the arms. Thin 12-μm tissue sections were obtained from a frozen sea star arm using a cryostat CM1510S (Leica Microsystems, Nanterre, France). The sections were then finger-thawed on an ITO-coated (indium tin oxide) glass slide (Bruker Daltonics, Bremen, Germany).

On-tissue MALDI and MALDI-MSI experiments

For MALDI-MSI, DHB was used at a concentration of 20 mg ml^{-1} in MeOH/water 60/40 (TFA 0.1 %). A liquid ionic matrix, DHB-DMA, was also tested at a DHB (1 ml) concentration of 20 mg ml^{-1} in MeOH/water 70/30 (TFA 0.1 %) mixed with 3.2 μl of pure (liquid) DMA as described by Snovida et al. [47]. The matrix solution was then sprayed on the tissue surface as micro droplets using an automatic system (ImagePrep, Bruker Daltonics, Bremen, Germany) or a modified electrospray nebulizer attached to a 500-μl syringe and the liquid flow rate set to 5 μl/min and an air flow to 3 l/min. The nebulizer was moved uniformly across the tissue surface for 15 min to ensure uniform matrix deposition. After deposition of the selected matrix, the images were acquired using an UltraFlex II MALDI-TOF/TOF mass spectrometer equipped with a Smartbeam II (Nd-YAG, 355 nm) laser having a repetition rate up to 200 Hz (Bruker Daltonics). MS spectral images were acquired in the negative ionization mode, and a mass-to-charge (*m*/*z*) range of 500–2000 was selected for the MALDI-MS spectra. A total of 500 spectra were acquired at each spot at a laser frequency of 200 Hz. Different spatial resolutions were selected. For the global images of the sea star arms, the spatial resolution was set to 120×120 μm^2, whereas for the detailed images, the spatial resolution was set to 40×40 μm^2. FlexImaging 3.0 software (Bruker Daltonics) was used for molecular image reconstruction. After MSI experiments, matrix was removed by successive ethanol bath and the sections were stained for histology (see ESM for details on the histological staining protocol).

MALDI-MS extract analysis

Mucus and body wall saponin extracts were analyzed with a Waters Q-ToF Premier mass spectrometer. The MALDI source is constituted of a Nd-YAG laser, operating at 355 nm with a maximum pulse energy of 104.1 μJ delivered to the sample at 200 Hz repeating rate. All samples were prepared using a mixture of 1 ml of a 100 mg ml^{-1} solution of DHB in water/acetonitrile (*v*/*v*) with 20 μl of DMA as the matrix [47]. The sandwich method was selected to prepare the sample/matrix co-crystal on the target plate. In this method, the saponin extract is not premixed with the matrix. A sample droplet (1 μl) is applied on top of a fast-evaporated matrix-only bed, followed by the deposition of a second layer of matrix in solvent (1 μl). The sample is then basically

sandwiched between the two matrix layers. The sandwich deposit was selected to obtain a more homogeneous co-crystal surface. For the recording of the single-stage MALDI-MS spectra, the quadrupole (rf-only mode) was set to pass ions between *m/z* 250 and 1500 and all ions were transmitted into the pusher region of the time-of-flight analyzer where they were mass-analyzed with a 1-s integration time.

Results and discussion

As the starting point of the present report, it is probably important to remind that we already investigated the saponins extracted from *A. rubens* [27]. In order to highlight the inter-organ and inter-individual variability, the saponin contents of different body components were separately analyzed by mass spectrometry. MALDI-TOF experiments were selected as the primary tool for a rapid screening of the saponin mixtures, whereas LC-MS techniques were used to achieve chromatographic separation of isomers. First of all, our analyses demonstrated a huge diversity of saponins. Secondly, the comparison of the saponin contents from the different body components revealed that each organ is characterized by a specific mixture of saponins [27]. As a typical example, the MALDI-TOF mass spectrum (negative ion mode) recorded on the aboral body wall extract (sea star of June 2014) is presented in ESM Fig. S1 and features signals that are attributed to saponin ions by associating the data from accurate mass measurements to the results of collision-induced dissociation experiments. Typical signals are detected at *m/z* 1211, 1227, 1241, 1243, 1257, and 1373. The identification of the corresponding saponin molecules can be achieved on the basis of Scheme 1. For instance, the ions detected at *m/z* 1211 can correspond either to Solasteroside A **1** or Ruberoside E **3**, keeping in mind that the observed ions correspond to deprotonated molecules, i.e., $[M\text{-}H]^-$. Scheme 1 gathers the 19 saponin molecules whose structures are fully described [27]. It is interesting to remind that, amongst those different congeners, epimeric (Solasteroside A **1** and Ruberoside E **3**), isomeric (Asterosaponin 1 **10**, Asteroside C **13**, and Ruberoside F **14**), and isobaric (Ruberoside A **9** and Glycoside B_2 **12**) saponins have been identified. Moreover, we have also detected additional saponin elemental compositions, i.e., $C_{57}H_{90}O_{27}S$ (*m/z* 1237), $C_{57}H_{92}O_{28}S$ (*m/z* 1255), and $C_{57}H_{94}O_{29}S$ (*m/z* 1273), without succeeding in the unambiguous identification of their structures [27]. Altogether, the saponin congeners of *A. rubens* are divided into 18 different elemental compositions (limited to 16 nominal masses) with 19 identified molecules (Scheme 1) and at least 7 additional molecules, still unknown [27]. In the present paper, we will only use the nominal masses to account for the presence of saponin ions, since the aim of our study is to demonstrate the general feasibility of saponin direct MALDI analysis on sea star tissues.

On-tissue MALDI-MS analysis of saponins

In direct connection with the MALDI-MS analysis of the saponin extract, we attempt to demonstrate that the analysis of saponins can be performed directly on the tissue without the need of extensive extraction and purification steps, except of course that a tissue section has to be prepared according to the procedure described in the experimental section. Such a procedure could then be considered as an alternative to the usual but time-consuming MALDI-MS analysis of saponin extracts.

When, in the context of MALDI-MSI (see below), numerous mass spectra are recorded for each point of the pixelated image, a mass spectrum averaging the data acquired on a specific region of the tissue section surface, for instance an organ, can be measured. It is very interesting to estimate if such a spectrum could reproduce the MALDI-MS mass spectrum of the saponin extract of this peculiar organ. We therefore compared the on-tissue MALDI-MS mass spectrum obtained by averaging the MS data for the aboral body wall (ABW) region and the classical MALDI-MS mass spectrum of the ABW extract obtained from the same animal (sea star of June 2014) (Fig. 1). On the MALDI-MS spectrum of the ABW extract, 16 intense signals are observed in the mass range *m/z* 1100–1500. The on-tissue MALDI-MS mass spectrum averaging the ABW data is clearly in close agreement with the conventional MALDI-MS analysis. A similar conclusion can also be derived when comparing the mass spectrum of the oral body wall (OBW) saponin extract and the on-tissue MALDI-MS mass spectrum averaging the MS data on this area (sea star of June 2014) (Fig. 2). Such a correlation is important for two reasons. First of all, the great qualitative and quantitative similarity between the on-tissue and after-extraction MALDI analyses confirms that the time-consuming saponin extraction procedure that is initiated by the dissection of the animals can be avoided by measuring directly on the tissue. Also, this similarity confirms that MALDI-MSI will be a reliable method to access the spatial distribution of saponins within the tissue.

MALDI-MSI of saponins on a whole sea star arm

One of our objectives is then to demonstrate that the spatial distribution of saponins within the organs can be determined directly on the tissue using MALDI-MSI methods. The preparation of the tissue section is described in the experimental part of the present report, but it is important to emphasize that, when compared to tissue preparation for MALDI-MSI targeting proteins, some typical steps (washing, organic treatment) are here eliminated to prevent the delocalization of the saponin molecules that are probably more prone to dissolution. Also in the case of sea star arm analysis, a major issue that must be overcome for the preparation of samples for MALDI-MSI study corresponds to the sectioning of the

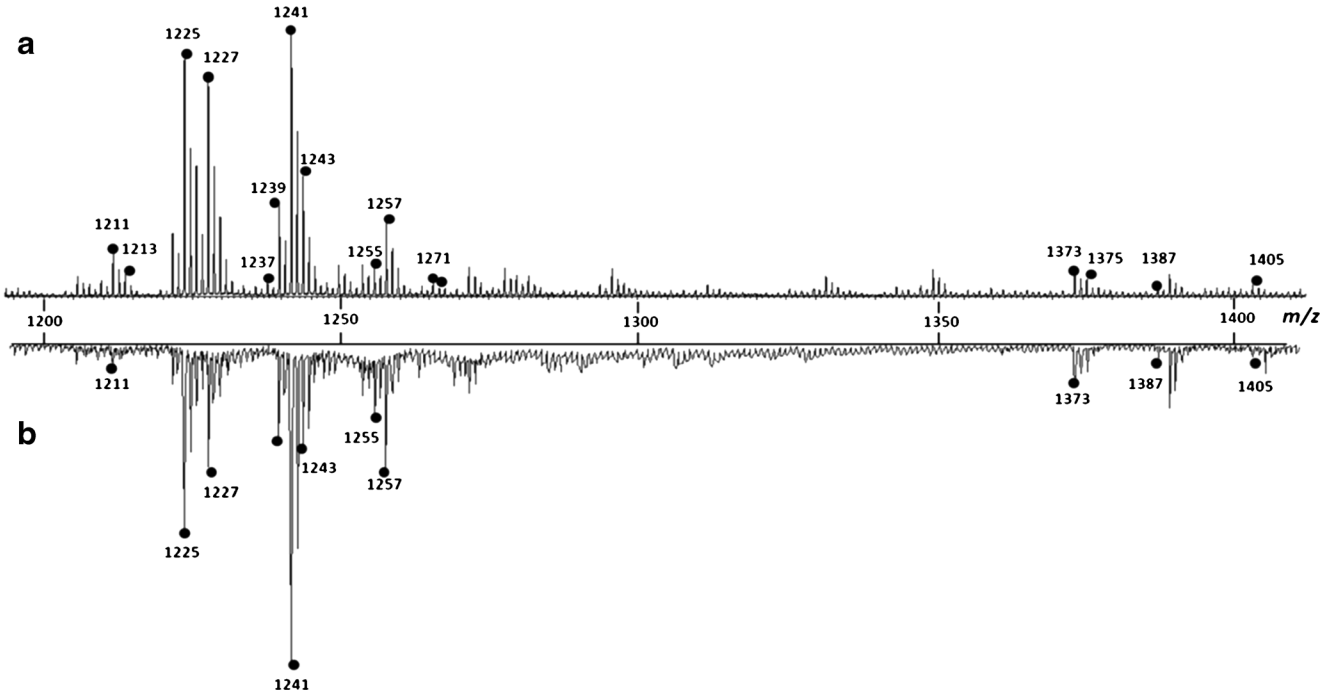

Fig. 1 Comparison of the MALDI-MS spectrum of the aboral body wall extract (**a**) and the MALDI-MSI spectrum of an aboral body wall area (**b**) for a sea star collected in June 2014. The MALDI-MSI analysis was performed on an embedded arm cross section. The classical MALDI-MS analysis was made on the sample after extraction and purification of saponins from the aboral body wall. Both analyses were obtained using the same laser frequency: 200 Hz. MS signals marked by a *black dot* correspond to saponin congeners already identified in *Asterias rubens* [27, 37]

tissue. Indeed, due to the presence of calcareous ossicles in the body wall, the preparation of a cross section of a complete sea star arm is already a real challenge. Our first attempts immediately revealed such a difficulty because the stiffness of

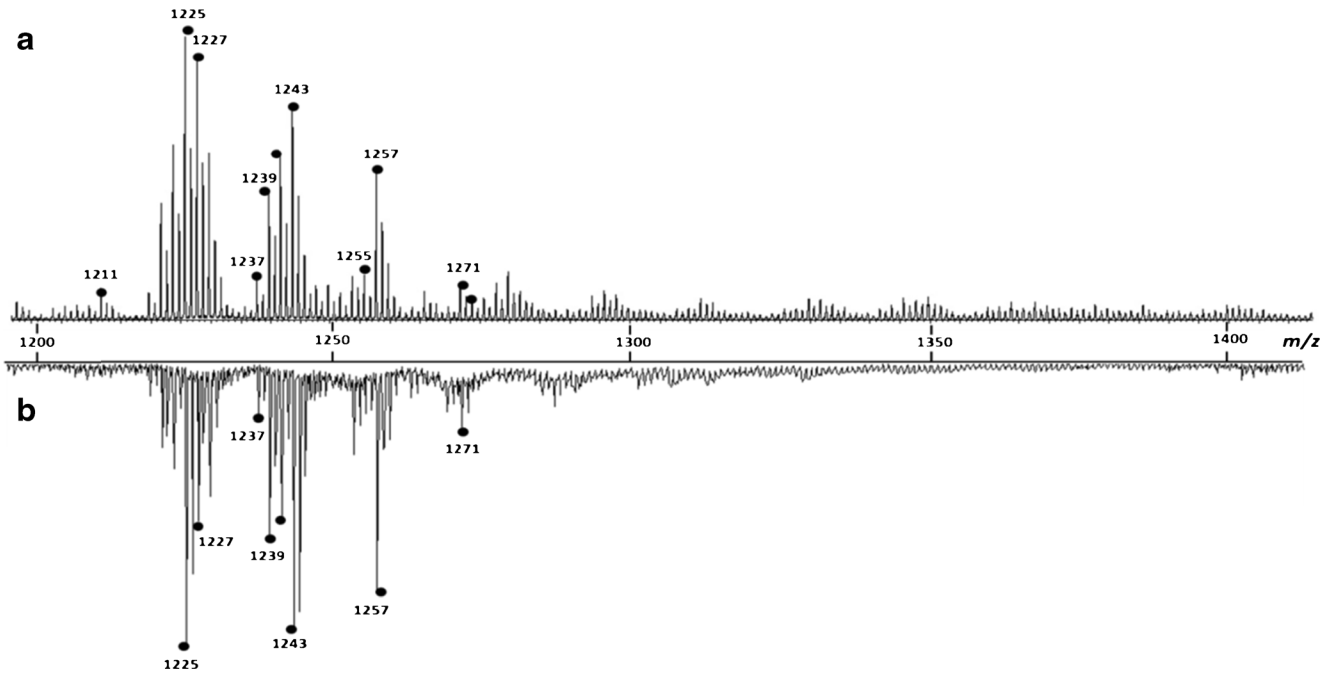

Fig. 2 Comparison of the MALDI-MS spectrum of the oral body wall extract (**a**) and the MALDI-MSI spectrum of an oral body wall area (**b**) for a sea star collected in June 2014. The MALDI-MSI analysis was performed on an embedded arm cross section. The classical MALDI-MS analysis was made on the sample after extraction and purification of saponins from the oral body wall. Both analyses were obtained using the same laser frequency: 200 Hz. MS signals marked by a *black dot* correspond to saponin congeners already identified in *Asterias rubens* [27, 37]

calcareous ossicles constituting the arm led to the loss of cohesion and the grinding of the softer organs during the sectioning process in the cryostat. Nevertheless, after numerous attempts, we managed to obtain a nice tissue section of the whole arm, but only for an organism collected in winter (see Fig. 3 for the histological pictures). Indeed, another aspect that must be taken into account for the sea stars is the relative development of the gonads and pyloric caeca according to the seasons. For example, in the case of the animals studied in the present work, the gonads and the pyloric caeca constituted about 9 and 7 %, respectively, of the total weight of the animal collected during winter 2012 (ESM Fig. S2). On the other hand, for the animal collected in summer 2012, i.e., after the reproduction period, the gonads constituted only 1 % of the total weight, whereas the caeca contribution increased to 14 %, confirming the collapse of the gonads after the reproduction season. Actually, another possibility to highlight the presence of cavities free of organs for the summer animals comes from the comparison between the global mass of organs for the dissected animals and the mass of the living animals. In the case of the winter animal, such a mass difference amounts to about 40 % and increases to 50 % for the summer animal. The mass difference is due to body fluids (mostly coelomic fluid) which are lost when the sea star is dissected, leaving empty spaces within the arms. Thus, due to the underdevelopment of the organs, especially the gonads, the cryosectioning process is likely to be even more difficult after the spawning season. In other words, the sectioning process is complicated by body wall crumpling when the sea star arms are empty if the gonads are undeveloped.

As a preliminary test, a matrix solution of DHB was deposited on the complete sea star (March 2012) arm section using an automatic vibration vaporization system (ImagePrep, Bruker Daltonics, Bremen, Germany) to cover the whole surface of the tissue section. In order to obtain a complete overview of the saponin distribution all across the arm cross section, the spatial resolution for this first image was fixed at $120 \times 120\ \mu m^2$. The recorded MALDI images are presented in Fig. 3 together with the histological pictures. At first glance, upon extraction of typical saponin ions such as *m/z* 1211, 1225, 1227, 1241, 1243, 1257, and 1373, the inhomogeneous distribution of saponin molecules across the tissue section is definitely confirmed, with saponin compositions being specifically detected in the aboral body wall (*m/z* 1211 and 1373) or

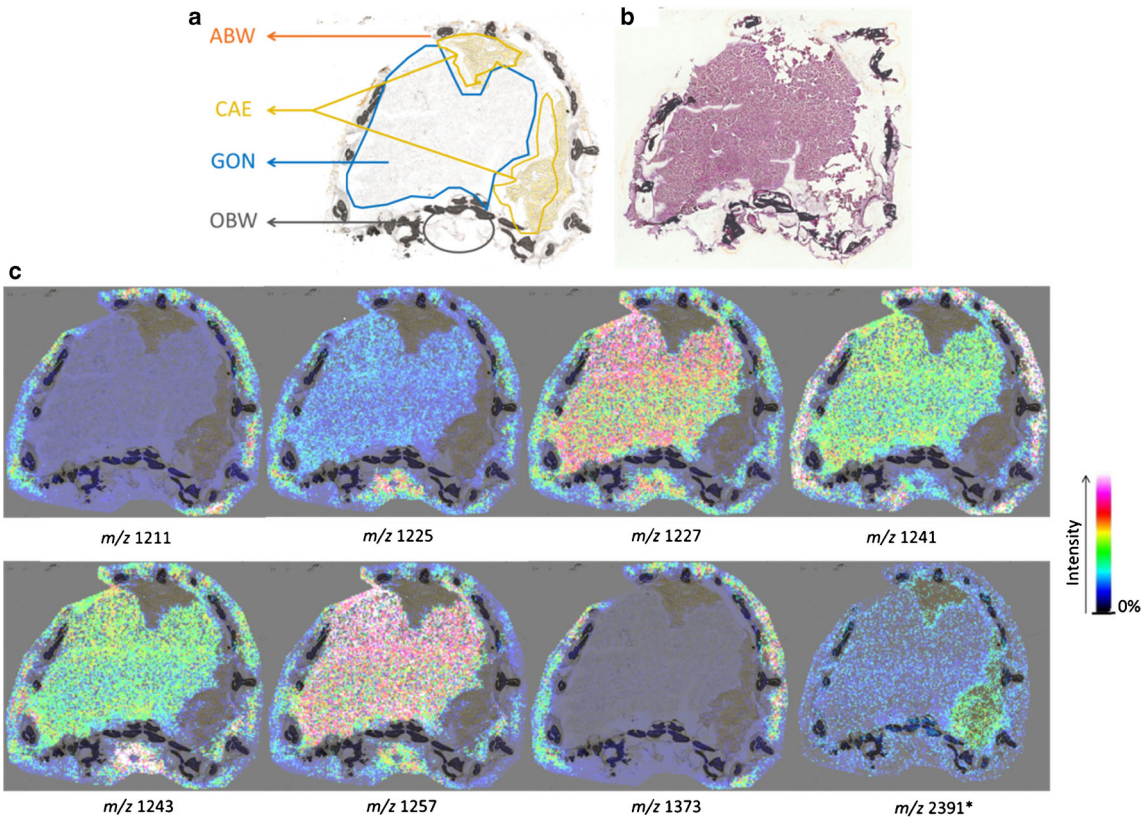

Fig. 3 MALDI-MSI data for the whole arm of the sea star *Asterias rubens* (no embedding) collected in March 2012. Scanned transverse section through the sea star arm without staining (**a**) and with the hemalum, phloxine, safran (HPS) staining (**b**). The arm diameter is about 25 mm. MALDI-MSI data with extraction of specific saponin ions and the *m/z* 2391 ions (**c**). The *color of the dots* reflects the intensity of the selected saponin ion signal. The *color ladder* of intensity begins in the lowest with the *black or dark blue* and grows towards the *pink or white*. *ABW* aboral body wall, *OBW* oral body wall (tube feet), *CAE* pyloric caeca, *GON* gonads. *Asterisk* the unidentified *m/z* 2391 ions are specifically observed in the CAE area

detected all across the tissue section (*m/z* 1243 for instance). A closer analysis further confirmed the data obtained in our previous paper regarding the inter-organ distribution of saponins. First of all, as unambiguously observed from Fig. 3, saponin molecules are scarcely detected in the pyloric caeca (CAE), since whatever the extracted mass-to-charge ratio, the CAE region remains dark. This is in close agreement with our previous data in which a really low hemolytic activity was measured for the CAE saponin extracts [27]. On the other hand, the presence of important amounts of saponins is confirmed within the gonads (GON), the aboral body wall (ABW), and the oral body wall (OBW; including tube feet), since all those areas appear bright red on the color-coded images when extracting mass-to-charge ratios corresponding to saponin ions. Ion suppression, that may ensue from the complex chemical environment of the tissue (CAE vs ABW, for instance) [48], could be responsible for the negligible saponin ion intensities in the CAE area. In order to establish whether such an effect has to be accounted for, we selected in the CAE region characteristic ions by exploring the MALDI mass spectrum (ESM Fig. S3). Beside saponin ions in the *m/z* 1100–1450 range, *m/z* 2391 ions are only observed in the CAE spectra but remain unidentified. In Fig. 3, the abundance of these *m/z* 2391 CAE ions is imaged on the whole arm cross section. The nice localization of those ions within the CAE region confirms that the low intensity of the saponin ions in the CAE area is probably due to the really low saponin concentration, in agreement with the low hemolytic activity of the CAE extract [27].

Some significant differences are then detected between the different organs. Indeed, the saponin ions recorded at *m/z* 1211 (Solasteroside A **1** and/or Ruberoside E **3**) and 1373 (Asteriidoside C **16**) are clearly specific to the ABW. This specificity was also established in our previous study [27]. Moreover, thanks to the color gradient, it is observed that some non-specific saponins are more abundant in a particular organ. This is the case for the saponins corresponding to the *m/z* 1241 ions, i.e., Ruberoside B **8** and/or saponin B **7**, which are clearly more abundant in the ABW. Furthermore, the *m/z* 1243 ions (Ruberoside A **9** and/or Glycoside B_2 **12**) and *m/z* 1225 ions (Ruberoside D **5**) are more representative of the tube foot (OBW) saponin content. Finally, the *m/z* 1227 ions, associated with Co-ARIS III (Ov. Asterosaponin 4) **15** and/or Regularoside B **2**, are more abundant in the gonads.

As already discussed, the MALDI-MSI and histological images presented in Fig. 3 were acquired on a tissue cryosection prepared from an animal sacrificed prior to the reproduction period (March 2012), i.e., characterized by arms filled with gonad tissues. For animals collected after the spawning period, all our attempts to obtain tissue sections systematically ended up with useless samples (see ESM Fig. S4 for a typical example). To overcome this issue, we decided to test carboxymethyl cellulose (CMC) as a filling substance to be injected in the empty arms prior to the cryogenisation step. Actually, previous studies have already demonstrated the real benefit of using embedding media for sectioning whole animal tissues [44]. From a practical point of view, the CMC filling clearly improved arm sectioning for all individuals, as exemplified by the transverse arm section presented in Fig. 4. CMC is shown to fill the empty spaces between organs affording a compact and cohesive block easier to cut (Fig. 4a). Nevertheless, one of the key aspects to establish, before claiming that such a CMC filling is efficient for the MALDI-MSI of sea star arms and similar samples, is that no diffusion of saponin molecules is occurring from the organs toward the CMC matrix. A global MALDI-MSI picture was recorded at a spatial resolution fixed at 120×120 μm^2 on a section obtained after CMC embedding, using similar matrix conditions to the previous analysis. A typical MALDI image is presented in Fig. 4 demonstrating that no significant diffusion of saponin molecules in CMC is observed. Indeed, for instance, the *m/z* 1211 saponin ions that are known to be specific of the ABW region are clearly observed at the expected localization (Fig. 4b). Additional MALDI-MSI images corresponding to other saponin ions are presented in the ESM (Fig. S5) and the comparison between the images in Fig. 1 (non embedded arm) and ESM Fig. S5 (embedded arm) affords further confirmation of the reliability of MALDI-MSI (with and without CMC) to probe the localization of saponin molecules within a section.

MALDI-MSI of saponins at higher spatial resolution

In a second phase of our development of the MALDI-MSI method to assess the intra-organ distribution of saponins inside the sea star arm, it quickly became unavoidable to increase the spatial resolution to better visualize the distribution of saponin congeners within the tissues. As a representative example, the distributions of saponin congeners within the ABW and the OBW regions of the sea star arm were targeted. In this context, a cross section through a CMC-embedded arm was prepared according to the procedure described in the previous section and in the experimental part. Based on recent literature, we selected a DHB/DMA liquid ionic matrix, since this type of matrix is known to afford a more homogeneous co-crystal surface [47]. The MALDI-MSI image was then acquired using a distance of 40 μm between two consecutive points and a spatial resolution of 40×40 μm^2. As revealed on Fig. 5 and ESM Fig. S6, the experimental procedure, i.e., CMC filling, cryosectioning, and liquid ionic matrix deposition, allows recording high-level MALDI images really helpful for the perfect localization of saponin molecules. For instance, the *m/z* 1241 and 1257 ions appear really abundant in the mass spectra recorded for the ABW and tube foot regions, respectively. Basically, those pieces of information were previously obtained by MALDI-TOF analysis of the saponin extracts of dissected and separated organs [27]. However, a

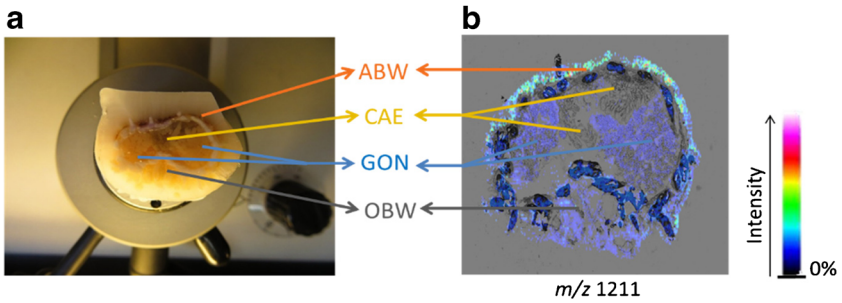

Fig. 4 The *left picture* shows the block of CMC with the embedded arm piece, stuck on the specimen holder of the cryostat with the Tissue-Tek OCT (**a**). *On the right*, MALDI image of the whole arm of a sea star (September 2012) with the CMC as embedding medium. The MALDI image represents the distribution of the saponin ion *m/z* 1211 (**b**). The arm diameter is about 25 mm. *ABW* aboral body wall, *OBW* oral body wall, *CAE* pyloric caeca, *GON* gonads

closer analysis of the recorded images (Fig. 5) points to the fact that the saponin molecules seem to be present mostly at the outer surface of the organ, rather being located inside the organs. To the best of our knowledge, this is the very first observation of this localization. For the ABW region, saponin molecules are therefore clearly present in the mucus surrounding the body wall and in the epidermis, but absent in the dermis and in the mesothelium (i.e., inner epithelium) of the animal. The images in Fig. 5b, and in particular the data highlighting the spatial distribution of saponin related to *m/z* 1373 ions, clearly demonstrate that no significant diffusion of saponin molecules in CMC occurs. Even more interesting is the saponin localization in the OBW region. Indeed, the MALDI image reveals that saponins are definitely localized outside the tube feet, probably in the oral mucus, but neither inside the disk nor the stem tissues (compare the stained histological section and MALDI images in Fig. 5 for a description of tube foot morphology). In order to assess the reproducibility of MALDI-MSI to probe saponin localization, additional images (40×40 μm^2) from another animal (female collected in February 2014) were recorded and are presented in Fig. S7 in the ESM. The presence of saponin molecules essentially in the mucus layer surrounding the tube feet is confirmed.

Qualitative and semi-quantitative analysis of body wall and mucus extracts

Based on the high-resolution MALDI-MSI analysis presented in Fig. 5, we propose that saponin molecules are probably present in the mucus surrounding the ABW and the OBW rather than inside the tissue. Nevertheless, to reach such a conclusion, we implicitly assume that, if saponin molecules are present inside the body wall tissues, their eventual entanglement does not prevent the molecules to be analyzed by MALDI at various extents, i.e., from no detected ions to weak ion current. Also, the origin of saponin molecules within the mucus will clearly remain questionable if no saponin

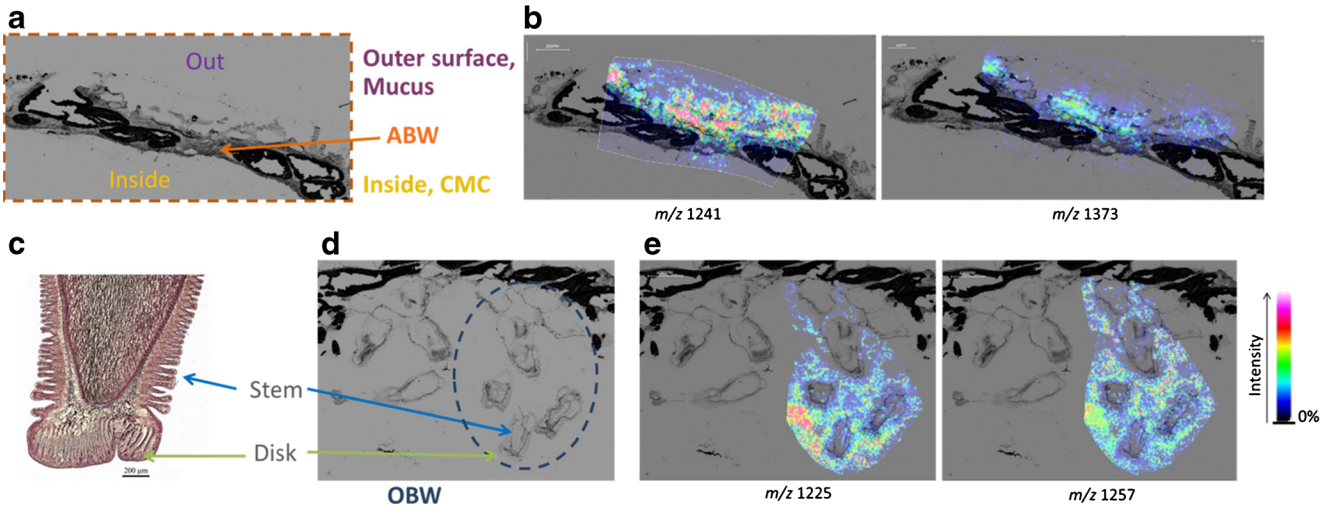

Fig. 5 MALDI-MSI analysis (CMC embedding) of a transverse section through the sea star arm (June 2014) with a zoom on the aboral body wall ABW (**a**) and the oral body wall OBW (tube feet with a diameter of about 1 mm) (**d**). The picture **c** corresponds to a light microscopy image of a longitudinal section through a tube foot showing the stem and the disk, stained with Heidenhain azan. The MALDI image **b** represents the distribution of the saponin ions *m/z* 1241 and *m/z* 1373 in the ABW and the MALDI image **e** the distribution of the *m/z* 1225 and *m/z* 1257 ions in the OBW (tube feet)

molecules are detected within the body wall tissues, either on the aboral or oral side. To get some further insight, we decided to address the problem by performing two different kind of analysis, one qualitative and one semi-quantitative, of the body wall saponin content.

First, we performed a qualitative analysis by measuring the MALDI mass spectra of saponin extracts from three complementary samples, i.e., collected mucus, body wall cleaned off mucus, and intact body wall (i.e., with mucus). Mucus samples, from separated ABW and OBW, were collected directly on 20 living animals by suction. All the mucus samples were pooled and their saponin content was extracted as described in ESM. As far as the intact/cleaned ABW/OBW samples are concerned, two different sea stars presenting the same characteristics, i.e., collected at the same period and site and presenting similar sizes and weights, were selected. For the sake of information, it is important to note that both animals were collected in summer without any possibility to make a distinction between male and female. But, we already demonstrated that the saponin content between males and females is only differing as far as the gonads are concerned, and that the body wall extracts are not significantly different between males and females at the same period of the year [27]. For one sea star (I1), we used the saponin extracts obtained from the ABW/OBW without any mucus removal. For the second sea star (I2), the mucus layers around the body wall were extensively removed by suction. MALDI-TOF measurements were performed on all the saponin extracts, from the ABW/OBW samples (with and without cleaning) and from the collected ABW/OBW mucus samples. Fig. S8A in the ESM unambiguously confirms that saponin molecules are present within the ABW mucus. Moreover, identical saponin profiles are also detected in the intact and cleaned ABW extracts (ESM Figs. S8B and S8C) (see ESM Fig. S9 for the OBW case). This observation points to the presence of saponin molecules in both the body wall tissues and the surrounding mucus.

It is well known that the use of MALDI-MS measurements for quantitative analysis is more than hazardous, given the great difficulty to get perfectly homogeneous samples on the target plate. In a second semi-quantitative approach, we therefore assessed the relative amount of saponin molecules within the different body wall extracts by measuring the hemolytic activity of the saponins samples against cow blood erythrocytes, according to a procedure described in one of our previous papers [27–49]. For comparison purposes, the hemolytic activities presented in ESM Fig. S10 are normalized according to the weight of the sample. First of all, we can already observe that the saponin concentration is higher on the aboral side relative to the oral side for both the non-cleaned (I1) and the cleaned (I2) individuals. Actually, to be really accurate, we can just conclude that the saponins from the aboral side present a higher cytotoxic activity because of a higher concentration or because of the presence of more active saponin congeners, compared to the oral side. In addition, these measurements clearly reveal that the saponin content is strongly modified when the mucus is removed. Indeed, approximately half of the hemolytic activity is lost upon mucus removal. This strongly correlates with the qualitative analysis since the presence of saponin molecules both inside the tissue and within the surrounding mucus is confirmed.

Interestingly, the saponin distributions of the ABW and ABW mucus (ESM Figs. S8A and S8B) and of the OBW and OBW mucus (ESM Figs. S9A and S9B) are demonstrated to be similar between the tissue and the mucus on the same side of the animal, but different from the aboral and the oral sides of the animal. From a structure-activity relationship, we can hypothesize that OBW and ABW saponin congeners could participate in the defense of the sea star against bacteria or other parasites. The different saponin distributions between the ABW and the OBW would then suggest that the sea stars have to face different external aggressions on both sides. Alternatively, the saponins of the OBW could be involved in another function, e.g., locomotion or temporary adhesion by the tube feet [50]. The similarity between the saponin content in the mucus and the body wall tissue on the aboral or the oral side indicates that the saponin molecules are produced specifically in the cells of the organs where they play their biological activities (i.e., the epidermal cells in the case of the body wall).

Conclusions

Asterosaponins are well-known secondary metabolites of the common sea star *A. rubens* in which they would be involved in chemical defense, digestion, and reproduction. Previously, using different mass spectrometry methods (MALDI-MS, LC-MS, MSMS), we observed significant differences in the distribution of the saponin ions between the different organs of the sea star (aboral body wall, tube feet, stomach, pyloric caeca, and gonads). In the present paper, we demonstrate that mass spectrometry molecular imaging by MALDI, i.e., MALDI-MSI, represents a powerful method to determine the spatial distribution of saponins directly on the tissue. Indeed, MALDI analysis of saponins can be performed directly on the tissue without the need of time-consuming extraction and purification procedures since the recorded on-tissue MALDI mass spectra are observed to reproduce the MALDI-TOF data obtained from the saponin extracts. MALDI imaging

methods also afford nice data on the distribution of saponin molecules within the organs. In this context, we also showed the advantage of using carboxymethyl cellulose as an embedding medium to facilitate the cryosectioning procedure. This step is especially critical in sea stars, whose arms are difficult to section because their body wall contains calcareous ossicles. MALDI-MSI performed at different spatial resolutions reveals that the inter- and intra-organ distributions of saponin congeners are not homogeneous, paving the way for future elegant structure/activity relationship investigations. For instance, we highlight that saponin molecules are located not only inside the body wall of the animals but also within the mucus layer, where they probably protects the animal against external aggressions.

Acknowledgments The MS laboratory acknowledges the "Fonds de la Recherche Scientifique (FRS-FNRS)" for its contribution to the acquisition of the Waters Q-ToF Premier Mass Spectrometer. E.H. and P.F. are, respectively, Postdoctoral Researcher and Research Director of the FRS-FNRS. M.D. is grateful to the F.R.I.A. for financial support. This work was supported by the FRFC research project no. T.0056.13 and in part by the EU FP7-OCEAN Project "Low-toxic cost-efficient environment-friendly antifouling materials" (BYEFOULING) under Grant Agreement no. 612717.

Conflict of interest The authors declare that they have no competing interests.

References

1. Li R, Zhou Y, Wu Z, Ding L (2006) ESI-Qq TOF-MS/MS and APCI-IT-MS/MS analysis of steroid saponins from the rhizomes of *Dioscorea panthaica*. J Mass Spectrom 41:1–22
2. Mackie AM, Turner AB (1970) Partial characterization of biologically active steroid glycoside isolated from the starfish *Marthasterias glacialis*. Biochem J 117:543–550
3. Kitagawa I, Kobayashi M (1977) On the structure of the major saponin from the starfish *Acanthaster planci*. Tetrahedron Lett 10: 859–862
4. Nigrelli RF (1952) The effect of holothurin on fish, and mice with sarcoma 180. Zoologica 37:89–90
5. Yamanouchi T (1955) On the poisonous substance contained in holothurians. Publ Seto Mar Biol Lab 4:183–203
6. Kubanek J, Pawlik J, Eve T, Fenical W (2000) Triterpene glycosides defend the Caribbean reef sponge Erylus formosus from predatory fishes. Mar Ecol Prog Ser 207:69–77
7. Kubanek J, Walen K, Engel S, Kelly S, Henkel T, Fenical W, Pawlik J (2002) Multiple defensive roles for triterpene glycosides from two Caribbean sponges. Oecologia 13:125–136
8. Van Dyck S, Gerbaux P, Flammang P (2009) Elucidation of molecular diversity and body distribution of saponins in the sea cucumber Holothuria forskali (Echinodermata) by mass spectrometry. Comp Biochem Physiol B Biochem Mol Biol 152:124–134
9. Bondoc KG, Lee H, Cruz LJ, Lebrilla CB, Juinio-Menez MA (2013) Chemical fingerprinting and phylogenetic mapping of saponin congeners from three tropical holothurian sea cucumbers. Comp Biochem Physiol B Biochem Mol Biol 166:182–193
10. Bahrami Y, Franco CMM (2015) Structure elucidation of new acetylated saponins, lessoniosides A, B, C, D, and E, and non-acetylated SAponins, lessoniosides F and G, from the viscera of the sea cucumber Holothuria lessoni. Mar Drugs 13:597–617
11. Maier M (2008) Biological activities of sulfated glycosides from echinoderms. Stud Nat Prod Chem 35:311–354
12. D'Auria MV, Minale L, Riccio R (1993) Polyoxygenated steroids of marine origin. Chem Rev 93:1839–1895
13. Hostettmann K, Martson A (1995) Chemistry & pharmacology of natural products, Saponins. Cambridge University Press
14. Prokof'eva NG, Chaikina EL, Kicha AA, Ivanchina NV (2003) Biological activities of steroid glycosides from starfish. Comp Biochem Physiol B Biochem Mol Biol 134:695–701
15. Stonik VA, Kalinin VI, Avilov SA (1999) Toxins from sea cucumbers (holothuroids): chemical structures, properties, taxonomic distribution, biosynthesis and evolution. J Nat Toxins 8:235–248
16. Kalinin VI, Prokofieva NG, Likhatskaya GN, Schentsova EB, Agafonova IG, Avilov SA, Drozdova OA (1996) Hemolytic activities of triterpene glycosides from the holothurians order dendrochirotida: some trends in the evolution of this group of toxins. Toxicon 34:475–483
17. Jorg MA, Vera K, Sven BA, Soren B (2011) Molecular activities, biosynthesis and evolution of triterpenoid saponins. Phytochemistry 72:435–457
18. Burnell DJ, Apsimon JW (1983) Echinoderm Saponins. Mar Nat Prod 5:287–389
19. Kalinin VI, Anisimov MM, Prokofieva NG, Avilov SA, Afiyatullov SH, Stonik VA (1995) Biological activities and biological role of triterpene glycosides from holothuroids. Echinoderm Studies Balkerma, Rotterdam, pp 139–181
20. Bordbar S, Anwar F, Saari N (2011) High-value components and bioactives from sea cucumbers for functional foods—a review. Mar Drugs 9:1761–1805
21. Mayo P, Mackie AM (1976) Studies of avoidance reactions in several species of predatory British Seastars (Echinodermata: Asteroidea). Mar Biol 38:41–49
22. Harvey C, Garneau FX, Himmelman J (1987) Chemodetection of predatory seaster Leptasterias Polaris by whelk Buccinum undatum. Mar Ecol Prog Ser 40:79–86
23. Mackie AM, Lasker R, Grant PT (1968) Avoidance reactions of mollusc Buccinum undatum to saponin-like surface-active substances in extracts of thenstarfish *Asterias rubens* and *Martasterias glacialis*. Comp Biochem Physiol B Biochem Mol Biol 26:415–428
24. Barkus G (1974) Toxicity in holothurians: a geographical pattern. Biotropica 6:229–236
25. Garneau FX, Harvey C, Simard SL, Apsimon J, Burnell D, Himmelman J (1989) The distribution of asterosaponins in various body components of starfish *Leptasterias Polaris*. Comp Biochem Physiol B Biochem Mol Biol 92:411–416
26. Kisha AA, Ivanchina NV, Kalinovsky AI, Dmitrenok PS, Stonik VA (2001) Sulfated steroid compounds from the starfish *Aphelasterias japonica* of the Kuril population. Comp Biochem Physiol B Biochem Mol Biol 128:43–52
27. Demeyer M, De Winter J, Caulier G, Eeckhaut I, Flammang P, Gerbaux P (2014) Molecular diversity and body distribution of saponins in the sea star *Asterias rubens* by mass spectrometry. Comp Biochem Physiol B Biochem Mol Biol 168:1–11
28. Mackie AM, Singh H, Owen J (1977) Studies on the distribution, biosynthesis and function of steroidal saponins in echinoderms. Comp Biochem Physiol B Biochem Mol Biol 56:9–14
29. Voogt PA, Van Rheenen JWA (1982) Carbohydrate content and composition of asterosaponins from different organs of the sea star *Asterias rubens*: relation to their haemolytic activity and implications for their biosynthesis. Comp Biochem Physiol B Biochem Mol Biol 72:683–688

30. Voogt PA, Huiskamp R (1979) Sex-dependance and seasonal variation of saponins in the gonads of the starfish *Asterias rubens*: their relation to reproduction. Comp Biochem Physiol 62:1049–1055
31. Van Dyck S, Caulier G, Todesco M, Gerbaux P, Fournier I, Wisztorski M, Flammang P (2011) The triterpene glycosides of Holothuria forskali: usefulness and efficiency as a chemical defense mechanism against predatory fish. J Exp Biol 214:1347–1356
32. Caulier G, Flammang P, Gerbaux P, Eeckhaut I (2013) When a repellent becomes an attractant: harmful saponins are kairomones attracting the symbiotic Harlequin crab. Sci Rep 3:1–5
33. Thomas GE, Gruffydd LLD (1971) The types of escape reactions elicited in the scallop Pecten maximus by selected sea-star species. Mar Biol 10:87–93
34. Naruse M, Suetomo H, Matsubara T, Sato T, Yanagawa H, Hoshi M, Matsumoto M (2010) Acrosome reaction-related steroidal saponin, Co-ARIS, from the starfish induces structural changes in microdomains. Dev Biol 347:147–153
35. Caprioli RM, Farmer TB, Gile J (1997) Molecular imaging of biological samples: localization of peptides and proteins using MALDI-TOF MS. Anal Chem 69:4751–4760
36. Franck J, Arafah K, Elayed M, Bonnel D, Vergara D, Jacquet A, Vinatier D, Wisztorski M, Day R, Fournier I, Salzet M (2009) MALDI imaging mass spectrometry, state of the art technology in clinical proteomics. Mol Cell Proteomics 8: 2023–2033
37. Sandvoss M, Huong Pham L, Levsen K, Preiss A (2000) Isolation and strucural elucidation of steroid oligoglycosides from the starfish *Asterias rubens* by means of direct online LC-NMR-MS hyphenation and one- and two-dimensional NMR investigations. Eur J Org Chem 7:1253–1262
38. Sandvoss M, Weltring A, Preiss A, Levsen K, Wuensch G (2001) Combination of matrix solid-phase dispersion extraction and direct on-line liquid chromatography-nuclear magnetic resonance spectroscopy-tandem mass spectrometry as a new efficient approach for the rapid screening of natural products: application to the total asterosaponin fraction of the starfish *Asterias rubens*. J Chromatogr A 917:75–86
39. Sandvoss M, Preiss A, Levsen K, Weisemann R (2003) Two new asterosaponins from the starfish *Asterias rubens*: application of a cryogenic NMR probe head. Magn Reson Chem 41:949–954
40. De Marino S, Iorizzi M, Palagiano E, Zollo F, Roussakis C (1998) Starfish saponins 55 isolation, structure elucidation, and biological activity of the steroid oligoglycosides from an Antartic starfish of the family Asteriidae. J Nat Prod 61:1319–1327
41. Kornprobst JM, Sallenave C, Barnathan G (1998) Sulfated compounds from marine organisms. Comp Biochem Physiol B Biochem Mol Biol 119:1–51
42. Riccio R, Iorizzi M, Minale L (1986) Starfish saponins isolation of sixteen steroidal glycosides and three polyhydroxysteroids from the mediterreanen starfish *Coscinasterias tenuispina*. Bull Soc Chim Belg 95:869–893
43. Tang HF, Yi YH, Li L, Sun P, Zhang SQ, Zhao YP (2005) Bioactive asterosaponins from the starfish *Culcita novaeguineae*. J Nat Prod 68:337–341
44. Nelson K, Daniels G, Fournie J, Hemmer M (2013) Optimization of whole-body Zebrafish sectioning methods for mass spectrometry imaging. J Biomol Tech 24:119–127
45. Hennebert E, Wattiez R, Waite JH, Flammang P (2012) Characterization of the protein fraction of the temporary adhesive secreted by the tube feet of the sea star *Asterias rubens*. Biofouling 28:289–303
46. Jangoux M, Vloebergh M (1973) Contribution à l'étude du cycle annuel de reproduction d'une population d'*Asterias rubens* (Echinodermata, Asteroidea) du littoral belge. Neth J Sea Res 6: 389–408
47. Snovida SI, Rak-Banville JM, Perreault H (2008) On the use of DHB/aniline and DHB/N, N-dimethylaniline matrices for improved detection of carbohydrates: automated identification of oligosaccharides and quantitative analysis of sialylated glycans by MALDI-TOF mass spectrometry. J Am Soc Mass Spectrom 19: 1138–1146
48. Heeren RMA, Smith DF, Stauber J, Kukrer-Kaletas B, MacAleese L (2009) Imaging mass spectrometry: hype or hope? J Am Soc Mass Spectrom 20:1006–1014
49. Van Dyck S, Gerbaux P, Flammang P (2010) Qualitative and quantitative saponin contents in five sea cucumbers from the Indian Ocean. Mar Drugs 8:173–189
50. Hermans C (1983) The duo-gland adhesive system. Oceanogr Mar Biol Annu Rev 21:283–339